

CosSGD: Nonlinear Quantization for Communication-efficient Federated Learning

Yang He¹, Maximilian Zenk², Mario Fritz¹

¹CISPA Helmholtz Center for Information Security, Saarbrücken, Germany

²German Cancer Research Center (DKFZ), Heidelberg, Germany

{yang.he, fritz}@cispa.saarland; m.zenk@dkfz-heidelberg.de

Abstract

Federated learning facilitates learning across clients without transferring local data on these clients to a central server. Despite the success of the federated learning method, it remains to improve further w.r.t communicating the most critical information to update a model under limited communication conditions, which can benefit this learning scheme into a wide range of application scenarios. In this work, we propose a nonlinear quantization for compressed stochastic gradient descent, which can be easily utilized in federated learning. Based on the proposed quantization, our system significantly reduces the communication cost by up to three orders of magnitude, while maintaining convergence and accuracy of the training process to a large extent. Extensive experiments are conducted on image classification and brain tumor semantic segmentation using the MNIST, CIFAR-10 and BraTS datasets where we show state-of-the-art effectiveness and impressive communication efficiency.

1. Introduction

Standard machine learning schemes require large-scale training data on a data center. To avoid such data centralization processes and allow users' participation during training, federated learning [5, 25] was proposed to enable mobile devices to update the shared model using their local data without uploading to the server, for improving the model performance and adapting to particular client groups.

Thanks to the careful designs of the configuration in federated learning, the system not only reduces communication costs by 10-100 \times compared to the naive distributed adaptation from the centralized stochastic gradient descent (SGD) but also preserves the high performance of learned prediction models. However, the communication bottleneck still constrains the widespread use of the learning pipeline [20], especially in the setup with large prediction models for pro-

viding higher performance and better services. Therefore, our focus in this work is to boost the trade-off between communication costs and model performance by effectively quantizing the gradients for client-to-server updates.

Quantization is widely utilized in federated or other distributed learning systems by linearly partitioning the data distribution into several intervals [2]. It is indeed able to reduce communication costs at a remarkable scale but lose model performance for exchange. Additionally, it is often combined with other approaches [17] for further reductions. In this work, we propose a new gradient quantization approach, referring to the SGD with our quantized gradients as CosSGD. Our approach is built on a cosine function, partitioning a space in a nonlinear manner. The quantization is fast in computation and needs little extra information for recovering the gradients. Therefore, the proposed nonlinear quantization is compatible with today's learning pipeline and other techniques, which can alternatively replace the previous gradients quantization methods [2, 17, 4].

The key property of our method is the nonlinearity, that we regard all the variables in a gradient vector differently. We focus on compressing the informative gradients more precisely, and approximating the less important values with larger errors. The philosophy of our method is different from previous works, that others try to obtain an unbiased quantization [2], to decrease the overall quantization errors with additional processing [40, 17], or to get compensations from the learning history [15]. In summary, the contributions of this work are as follows:

- We present a novel cosine-based quantization method for compressing gradients, which is rather simple and effective. There is no extra computation or compensational training signals required to keep the precision of gradients, which is affordable from constrained computation and communication conditions. Therefore, it is potentially to be used in a large variety of distributed learning systems.
- We show the quantized gradients are quite suitable to equip with data-driven lossless compression. The

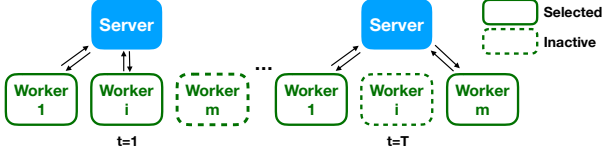


Figure 1: The federated learning scheme in this paper. In each round, the model on the server aggregates the updates from all the selected workers. A subset is selected to update the shared model in each training round.

compression allows further communication reduction compared to original float numbers, more significantly.

- Combining our nonlinear quantization with the lossless data compression [10] and previous sparsification method [17], we provide a federated learning system with negligible decreases in model performance under 200-1000+ compression ratios w.r.t gradients, compared with float32 based training. Finally, we report strong results on MNIST and CIFAR-10 for image classification, as well as the BraTS dataset for semantic segmentation of MRI volumes.

2. Related work

2.1. Federated learning from decentralized data

Federated learning (FL) is a distributed machine learning scheme, which has drawn a lot of attention in mobile services [12, 47] as well as privacy-sensitive applications [37, 36, 29]. A FL system [6] has many aspects and we discuss the learning methods. More comprehensive surveys can be found in [46, 21, 13, 20]. Federated averaging (FedAvg) [25] is a simple and popular method to update a shared model with weighted gradients from local computation nodes. In each communication round, a random subset of nodes (workers) is selected to perform computation on the local data and then return the gradients to the server/controller. FedAvg suggests doing more computation on each node (e.g., more training epochs, smaller batch size, etc) instead of exchanging the gradients frequently. In this way, models are able to converge with fewer communication rounds in various scenarios of data distributions, such as the Non-IID case. Besides, FL has been explored in the decentralized setup that there is not a central server [29, 19, 32], that imprecise training signal may spread widely and quickly through the connections between computation nodes. Recently, FL is improved with adaptive optimization. [30] applies an optimizer on the server with momentum terms to update the model with aggregated gradients, which shows faster convergence and higher performance in many tasks. Mime [14] uses server-level momentum in each client to mitigate the client-drift due to the data heterogeneity across different clients, reaching higher performance. FedCD [18] dynamically groups the local work-

ers with similar data distributions to improve the model performance on Non-IID data.

In this work, we study the centralized server-based federated learning under the FedAvg scheme [25], as shown in Figure 1. Different gradient compression techniques are compared to demonstrate the advances of the proposed quantization over prior work.

2.2. Gradients compression for improving communication efficiency

To improve communication efficiency, several efforts have been made, which fall into the following categories [27]: gradients sparsification, decomposition and quantization. Sparsification aims to return the parts of gradients including the main strategies of random locations [17], top-K locations [1, 39, 3, 22]. Further, Wangni et al. formulate the encoding of gradient vectors as a convex optimization problem to minimize the length of codes [44]. ScaleCom[7] leverages the similarity of gradient distribution in computation nodes to improve the gradient sparsification for scalable distributed learning. Decomposition-based approaches compress the gradients into a low-rank approximation with fewer data to deliver [17]. In addition, PowerSGD [43] computes the gradient approximation by a generalized power iteration [38], and reuse the approximation from the last training to avoid expensive decomposition at every step.

Our contribution belongs to the gradient quantization. The proposed method is compatible with previously existing techniques (i.e., sparsification) and fruitful in learning with highly compact data for communication, obtaining stronger performance at the same level of costs to others. Further, our solution is not only communication-efficient but also computation-efficient in which no extra computation is needed like matrix decomposition or other operations.

2.3. Gradients quantization

Quantization has a long history in signal processing for lossy data compression. Recently, it also had a crucial role in squeezing the model size from deep learning which needs millions of parameters [11, 9, 48, 23]. In federated learning, to reduce the worker-to-server communication costs, quantization techniques are applied to compress the gradients from original float numbers with low-bits representation. Due to the fact of biased approximation, systems may lose performance after quantization. To overcome this, two parallel work TernGrad [45] and QSGD [2] utilize probabilistic unbiased quantization with correct expectations for quantized gradients. In addition, quantization errors can be reduced by rotation operations with random Hadamard matrices, which needs extra computation [40]. Accordingly, communication efficiency is vastly improved

by combining with sparsification and improved quantization [17]. In particular, 1-bit compression schemes have been explored to reduce the communication cost significantly. Seide et al. [35] have pioneered the 1-bit compression for the communication-efficient distributed training of networks for speech recognition. signSGD [4] shows that the gradient signs – which can be compressed with 1-bit data – are strong training signals for optimizing non-convex problems with convergence guarantees. signSGD can be further improved with the error feedback from the previous training step [15].

Different from prior work, we design a nonlinear quantization, which is in particular effective in compressing gradients. Our approach provides precise and crucial training signals for the optimization on decentralized data. Last, our quantization does not need error feedback [15] to adjust the gradients; instead, we provide critical gradients independently in every step.

3. CosSGD: Optimization with a *cosine* based quantization

In order to achieve higher compression rates while still being able to successfully train federated models, we propose a new cosine based quantization scheme that better preserves the information critical to training. We first describe our method in this section and then discuss the properties of the nonlinear quantization. Lastly, we provide empirical studies to support our motivation and give an intuitive explanation of why our method is effective.

In federated learning or data-parallel optimization, a number of workers share the same model $M = (w_1, \dots, w_n)^T$ and update it by local data without explicit interactions between workers. After learning with local data, the gradients for the parameters ∇M are sent to the server. Accordingly, the model is updated by aggregating the gradients [25] from all the selected workers $\{\nabla M_i\}_{i=1}^m$ with the following formulation:

$$M^{t+1} = M^t - \eta_s \cdot \frac{\sum_{i=1}^m \nabla M_i \cdot N_i}{\sum_{i=1}^m N_i} \quad (1)$$

to update the model at time step t , where $\{N_i\}_{i=1}^m$ are the numbers of training data on individual workers and η_s is the learning rate on the server.

To reduce the worker-to-server communication costs, we utilize quantization on the gradients ∇M . The direction of gradients can be depicted by the a set of variables, or the angles of the gradient to the standard coordinate. Therefore, we try to encode the angle information during quantization, which approximates the deepest gradient directions explicitly. Let $\mathbf{g} = \nabla M$ be the gradient vector, where $\mathbf{g} = (g_1, \dots, g_n)^T$. The angle between the gradient vector

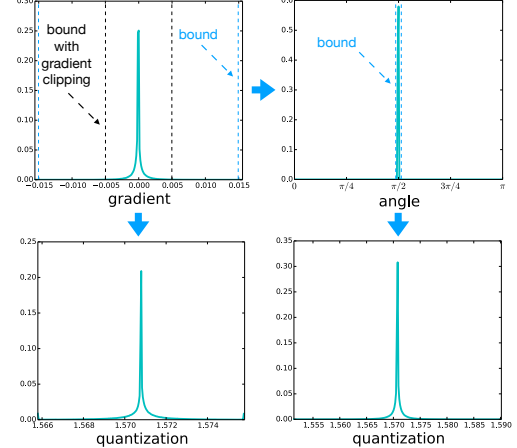


Figure 2: An example of the gradients histogram from the CNN on CIFAR-10 and our quantization results. We compute the angle bound to avoid the waste of quantization intervals (top-right). We alternatively perform gradient clipping on top gradients (top-left).

and i^{th} axis $\mathbf{a}_i = (\underbrace{0, \dots, 0}_{i-1}, 1, 0, \dots, 0)^T$ is computed by the inner product:

$$\cos(\theta_i) = \frac{\mathbf{g}^T \mathbf{a}_i}{\|\mathbf{g}\|_2 \cdot 1} = \frac{g_i}{\|\mathbf{g}\|_2}. \quad (2)$$

Accordingly, $\theta_i = \arccos(\frac{g_i}{\|\mathbf{g}\|_2})$, where $\theta_i \in [0, \pi]$. Different to previous linear-based uniform quantization [2, 17], we quantize each value in a gradient vector on the angle θ instead of the original values or the linearly transformed values [40] in the Euclidean space. Specifically, in a normalized gradient vector, there are very few or even no values close to 1 or -1, especially when the dimension of the gradient is high. Therefore, we will not quantize the angle vector $\Theta = (\theta_1, \dots, \theta_n)^T$ on $[0, \pi]$; instead we compute a bound $b_\theta = \min(\min(\Theta), 1 - \max(\Theta))$ and quantize Θ on $[b_\theta, \pi - b_\theta]$, as shown in Figure 2. The bound facilitates a more precise quantization in that it avoids the waste of quantization bins for the place where there is no value distributed. In addition to the automatic computation of b_θ , we have tried manually set on it. Sometimes, there is one dimension dominating the gradient vector. It will lead to a very large b_θ , whereas most gradients are small. Hence, the intensely dominated gradients prevent others from making full use of the quantization space. To avoid this situation, we apply the gradient clipping on the top ones as an alternative solution to get the bound b_θ , as shown in Figure 2. At the end, our quantization is a nonlinear operation that the space is partitioned unequally for the whole distribution.

The above quantization for gradients, referred to Q_g , is built on Q_θ for angles and biased, because $\mathbb{E}(Q_\theta(\Theta)) \neq \Theta$. In [2, 45], an unbiased quantization is achieved according to a probabilistic procedure. Likewise, our cosine-based quan-

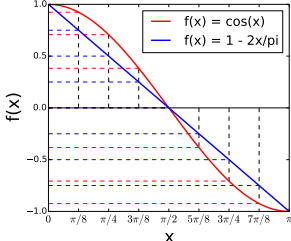


Figure 3: Comparison between different mappings in linear and our cosine-based quantization.

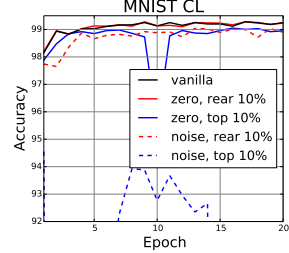


Figure 4: Results (%) of centralized learning (CL) on MNIST. The top gradients are more vital compared to the rears.

tization can be extended with the probabilistic scheme, satisfying the unbiasedness. Formally, our unbiased s -bits quantization is defined as

$$Q_\theta(\Theta; b, s) = \begin{cases} \lfloor v \rfloor & \text{with } 1 - p \\ \lfloor v \rfloor + 1 & \text{otherwise,} \end{cases} \quad (3)$$

where $v = \frac{\Theta - b}{\pi - 2b} \times (2^s)$, $p = v - \lfloor v \rfloor$, and $\lfloor \cdot \rfloor$ is the round down operator. Finally, both our biased and unbiased methods return a quantized vector $Q_\theta(\Theta)$, the norm of the original gradient vector $\|\mathbf{g}\|_2$, and the bound b_θ . The gradients can be computed on the server by reversing the process.

3.1. Property of our quantization

Quantization error bound. As depicted above, we quantize the angle vector Θ over $[b_\theta, \pi - b_\theta]$. Due to the symmetric property of the cosine function on $[b_\theta, \pi - b_\theta]$, we focus on analyzing our biased quantization in the range of $[b_\theta, \frac{\pi}{2})$, and the left holds the same rule on an opposite direction. The unbiased version can be estimated by taking the expectation form into considerations.

The angle bound b_θ corresponds to a gradient bound b_g (i.e., $g_i \in [-b_g, b_g]$), where $b_\theta = \arccos(\frac{b_g}{\|\mathbf{g}\|_2})$. Let $q = \frac{\pi - 2b_\theta}{2^s}$ be the width of angle quantization intervals, and then the quantization error of g_i is bounded by

$$\begin{aligned} |g_i - Q_g(g_i)| &\leq [\cos(q \cdot (k + \frac{1}{2})) - \cos(q \cdot (k + 1))] \cdot \|\mathbf{g}\|_2 \\ &= 2 \cdot \sin(q \cdot (k + \frac{3}{4})) \cdot \sin(q \cdot \frac{1}{4}) \cdot \|\mathbf{g}\|_2, \end{aligned} \quad (4)$$

where $k = \lfloor (\arccos(\frac{g_i}{\|\mathbf{g}\|_2}) - b_\theta)/q \rfloor$, because $\cos(\theta - \epsilon) - \cos(\theta) < \cos(\theta) - \cos(\theta + \epsilon)$ on $[0, \frac{\pi}{2})$.

Observing the Eq. (4), we realize the quantization errors for different intervals are not fixed, as shown in Figure 3. Since $\sin(\cdot)$ is monotonically increasing on $[b, \frac{\pi}{2})$, the quantization errors $|g_1 - Q_g(g_1)| < |g_2 - Q_g(g_2)|$ if $|g_1| > |g_2|$. As a result, our method quantize the gradients

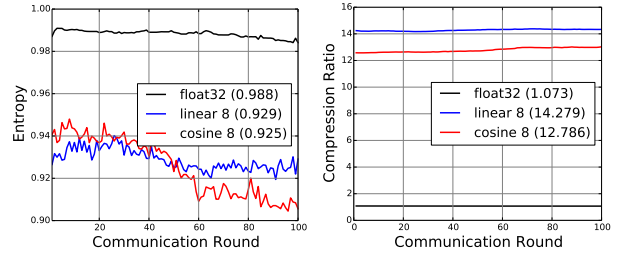


Figure 5: Statistics on the 8-bits compressed gradients on BraTS 2018. No random mask applied. The compression ratios for 8-bits quantized gradients are increased from $\sim 4\times$ to more than $12\times$ after applying the *Deflate* compression, while float32 is only compressed at $1.073\times$.

with larger magnitudes more precisely, which is important to training [33, 22].

Further, we then compare the quantization errors between the linear method and ours. The biased linear quantization has an error bound of $\frac{b_g}{2^s} = \frac{\cos(b_\theta)}{2^s} \cdot \|\mathbf{g}\|_2$ for all the gradients on $[-b_g, b_g]$, therefore, the condition for that the k -th quantization interval from our method has smaller errors than the linear is

$$2 \cdot \sin(q \cdot (k + \frac{3}{4})) \cdot \sin(q \cdot \frac{1}{4}) < \frac{\cos(b_\theta)}{2^s}. \quad (5)$$

In the Eq. (5), only variable k affects the condition, and we compute the number of intervals satisfying Eq. (5). From our computation, top 50%, 42.9% and 44.1% quantization intervals from our 2-, 4- and 8-bits compression have smaller error bounds than the linear method. Interestingly, even though the quantization errors from our method are larger than the linear for most variables in a gradient vector, we are able to show more favorable results. This observation and analysis is inspiring to help us understanding gradient quantization that the success of recovering larger gradients precisely plays an critical role for training.

Besides, our quantization also has an opposite observation to relevant work in model parameter compression [48], which learns finer quantization intervals for densely distributed ranges. However, the large gradients are rarely distributed, as an example shown in Figure 2. Consequently, we show compressing gradients requires considering the importance of gradients, instead of their distribution only.

1-bit quantization. The above quantization is flexible in which the trade-off between precision and compression ratio is allowed to be determined by applying the quantization at a variety number of bits. When we apply 1-bit compression, the angle vector $\Theta \in \{b_\theta, \pi - b_\theta\}$, and then the quantized gradient vector $Q_g(\mathbf{g}) \in \{a \cdot \|\mathbf{g}\|_2, -a \cdot \|\mathbf{g}\|_2\}$ where a is a scaling constant determined by the bound b_θ . In particular, we notice that our quantization degenerates to signSGD [4] if there is no bound and norm considered.

3.2. Empirical analysis

To demonstrate the importance of different gradients, we provide a toy study on the MNIST dataset with SGD for image classification, as shown in Figure 4. To have a more general observation, we consider centralized learning settings here. In each step, we set the top or the rear gradients to 0 by ordering their absolute values. We can observe that the blue solid line achieves less final performance and is not stable at the 10^{-th} epoch, while the red solid line has similar behavior to vanilla training. Similarly, we also add the Gaussian noise of standard deviation 0.1 on those gradients, as drawn with the dash lines. Figure 4 clearly indicates the gradients with larger absolute values are much more important than others. Less precision on the small gradients will not affect the learning procedure, in contrast, inaccurate large gradients lead to the failure of learning or poor performance very likely.

4. Interplay between quantization and lossless data compression

To further compress the data for low-cost communication, we apply the *Deflate* algorithm [10] on the quantized gradients before sending back, which is lossless data-dependent compression and widely used in such as gzip or png files. Even though we do not design a specific algorithm to encode the quantized gradients like [2], our solution is extremely simple and effective that the quantized gradients can be compressed significantly by the *Deflate*, whereas original float numbers are compressed slightly. From our observation, the gradients are mainly distributed near 0 which have similar binary codes in the memory. Hence, the binary stream for a quantized gradient has many repeated patterns, which can be compressed at a high degree. However, the binary codes for two very close float numbers can differ significantly. From this perspective, the quantization of gradients is important and necessary even there are other solutions to reduce the communication costs.

We provide statistics on the quantized gradients and original float gradients. Figure 5 shows the multi-scale entropy and the accumulated compression ratio curves on BraTS 2018 training. We can see the entropy for quantized gradients are smaller than float numbers in memory, indicating stronger potential compression capability. As a result, the *Deflate* gives further 3-4 \times cost reduction for 8-bits quantized gradients, and finally compresses gradients by more than 10 \times . Besides, we are interested in applying our quantization with previous successful techniques, which are parallel to ours. In our system, we utilize random masks [17] to send parts of the gradients, leading to extremely reduced communication costs while maintaining the high performance of trained models. In the end, we summarize our federate learning system in Algorithm 1.

Algorithm 1 Communication-efficient federate learning with s -bits based CosSGD and FedAvg [25]. E is the number of local epochs, B is the local batch size, and C is the percentage of selected local workers.

Input: Clients $\mathbb{I}_c = \{i_1, \dots, i_m\}$. A global model M_0 . Communication round T . Global and local base learning rates η_s and η_c .

Server:

```

1: Initialization of  $M_0$ ,  $\eta_s^* = \eta_s$  and  $\eta_c^* = \eta_c$ .
2: for each round  $t = 1 \dots T$  do
3:   Select a random subset  $\mathbb{I} \in \mathbb{I}_c$ , where  $|\mathbb{I}| = m \cdot C$ .
4:   for worker  $i$  in  $\mathbb{I}$  do
5:      $Q(\Theta_i)$ ,  $\|\mathbf{g}_i\|_2$ ,  $b_i$ ,  $N_i = \text{Worker}_i(M_{t-1}, \eta_c^*)$ 
6:     Decompress  $Q(\Theta_i)$  with Deflate [10].
7:      $\nabla M_i = \cos(Q(\Theta_i)) \cdot \frac{\pi - 2b_i}{2^s} + b_i \cdot \|\mathbf{g}_i\|_2$ 
8:   end for
9:   Update  $M_{t-1}$  and obtain  $M_t$  using Eq. (1).
10:  Update  $\eta_s^*$  and  $\eta_c^*$ .
11: end for
12: return  $M_T$ .
```

Worker:

```

1: Preparing  $N$  training examples.
2: Initialization of  $M^*$  and  $\eta_c^*$  from the input  $M_{in}$ .
3: for epoch  $i = 1 \dots E$  do
4:   for batch  $j = 1 \dots \lceil \frac{N}{B} \rceil$  do
5:      $M^* = M^* - \eta_c^* \cdot \nabla M^*$ 
6:   end for
7: end for
8:  $\mathbf{g} = M_{in} - M^*$  and compute  $\|\mathbf{g}\|_2$ .
9:  $\Theta = \arccos(\mathbf{g}/\|\mathbf{g}\|_2)$ 
10: Apply quantization, achieving  $Q(\Theta)$  and  $b$ .
11: Apply Deflate compression on  $Q(\Theta)$ .
12: return  $Q(\Theta)$ ,  $\|\mathbf{g}\|_2$ ,  $b$ ,  $N$ 
```

5. Experiments

We conduct our experiments of federated learning using FedAvg [25] on image classification with MNIST, CIFAR-10, and brain tumor semantic segmentation with BraTS2018 dataset. All the methods are implemented with PyTorch [28] and PySyft [34]. To test the broad optimization scenarios, we employ SGD [31, 41] or Adam [16] as the basic learners for the clients. Besides, we train the baseline models with float32 for the FedAvg, and apply gradients quantization with 8-, 4- and 2-bits compression. For all the training with quantization (i.e., the baselines and ours), we utilize layer-wise quantization on the neural networks. By default, we apply the biased quantization for ours and perform gradient clipping on top 1% gradients to obtain the bound b_θ as depicted in section 3.

Our nonlinear quantization is compared with the standard linear based method, linear based probabilistic unbiased quantization (refer to linear (U)) [2], as well as the improved version (refer to linear (U, R)) [17] with random Hadamard rotations for reducing quantization errors [40]. Finally, we also compare our method with 1-bit compressions, including signSGD [4], signSGD+Norm [43] (equivalent to our 1-bit compression), and signSGD with error feedback (EF-signSGD) [15].

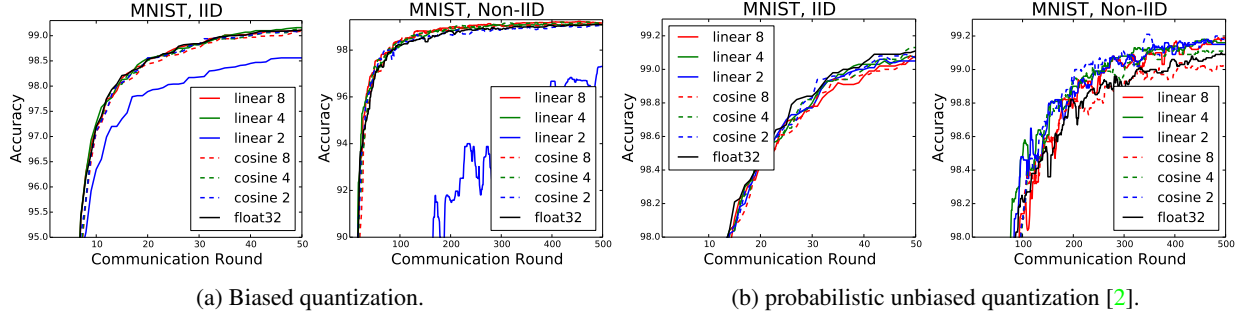


Figure 6: Comparison results (%) to linear quantization on MNIST ($B = 10, E = 1, C = 0.1$).

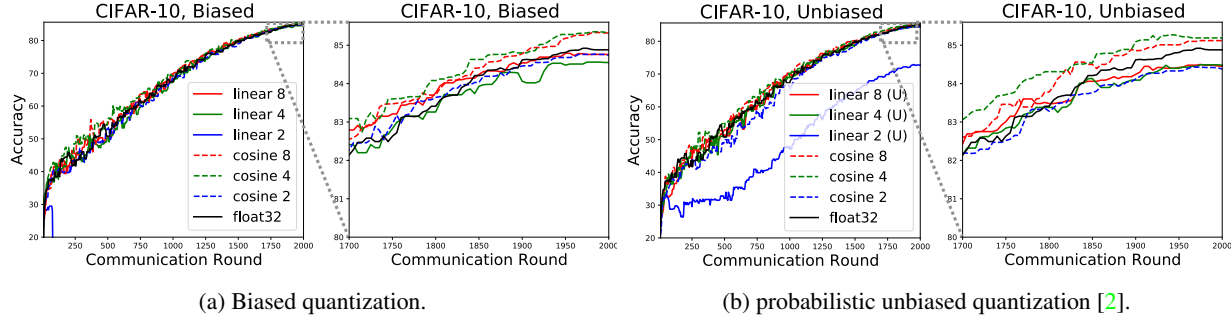


Figure 7: Comparison results (%) to linear quantization on CIFAR-10 ($B = 50, E = 5, C = 0.1$).

5.1. Datasets and setup

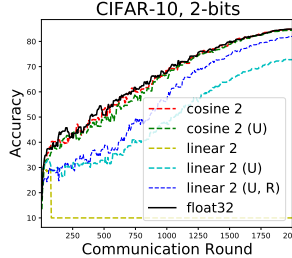
MNIST In this experiment, we utilize a CNN model with 1,663,370 parameters in total, with the same architecture as in [25]. In our setting, we apply **Non-IID** and **IID** data distribution to split the data for all the clients, that the Non-IID setup ensures each client is able to touch at most two classes of examples [25]. For both setups, we split the training set into 100 clients and each client has 600 training examples. In the local training, we set $E = 1$ and $B = 10$, and 10% ($C = 0.1$) workers are randomly selected to update and send the local gradients. Since Non-IID setup converges slower and thus needs more training iterations, we apply 500 and 50 communication rounds for the Non-IID and IID respectively. SGD (no momentum) is applied to each worker. Weight decay for local workers is set to 1e-4. Learning rate η_s is kept to be 1 for all the training. We apply fixed η_c as 0.1 for IID setup, and a cosine scheduler from 0.1 to 0 for Non-IID setup for the ease of choosing a learning rate.

CIFAR-10 Following previous work [25], we apply a CNN model [42] with 122,570 parameters, which consists of three convolution layers and two fully connected layers. We randomly split the whole training set into 100 partitions equally, and then we are able to reproduce the results with float32 based training reported in [25]. In detail, we apply 2000 communication rounds to train a model. For the FedAvg, we set $E = 5$ and $B = 50$, and $C = 0.1$. In local

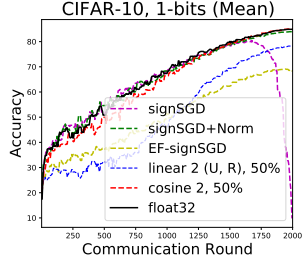
workers, SGD with momentum is applied, and the momentum term is set to 0.9. η_s is set to 1, and η_c is determined by the number of the communication round and a cosine scheduler from 0.1 to 0.

BraTS datasets We apply BraTS 2018/2019 to conduct experiments for brain tumor semantic segmentation using federated learning [37, 36]. As one of the goals of federated learning, medical applications put high importance on the protection of data privacy from multiple institutions and patients. We train a 3D-UNet [8] on BraTS 2018 training set [26], which includes 285 annotated MRI scans of 5 labels. The network has 9,451,567 parameters ($\sim 36.05\text{MB}$ with float32) and the architecture details will be depicted in the supplementary materials. We randomly partition the training set into 10 parts as local data (representing 10 hospitals), and aggregate the gradients from all the workers ($C = 1$) in each training round. Besides, we set $E = 3$ and $B = 3$ for the FedAvg, and the local training is accomplished with separate Adam optimizers with (0.9, 0.999) betas. BraTS 2019 contains 335 training examples, which covers the BraTS 2018 training set. Therefore, we train a model using the BraTS2018 training set and compute the dice score on the 50 examples from BraTS 2019 that are not seen during training.¹ For all the models, we apply 100 communication rounds to train. η_s is kept to be 1, and η_c is computed with cosine scheduler with warm restarts [24] at 20^{-th} and 60^{-th} round.

¹BraTS datasets do not provide GT for the validation set.



(a) Two-bits.



(b) One-bit in average.

Figure 8: Low-bits comparison results (%) to various compression schemes on CIFAR-10 ($B = 50, E = 5, C = 0.1$).

5.2. Comparison with previous methods

First of all, we compare our nonlinear quantization with previous linear quantization [2] and the improved version [17]. Besides, we also compare the biased quantization without the probabilistic regime. Even though the probabilistic regime will not bring expensive extra computation, and it will be used in practice. However, the evaluation of biased versions is still interesting to compare different quantizations, providing an initial understanding of the methods with different types of quantization intervals.

Figures 6 and 7 show the results for MNIST and CIFAR-10. From the subfigures (a) in them, we can clearly see the 2-bits biased linear quantization fails to successfully train a model, obtaining models either with unsatisfied results or not converged. After applying the probabilistic regime, improved results are obtained in the subfigures (b) of Figure 6, 7. However, the unbiased linear-based 2-bits compression in Figure 7 (b) is still worse than ours with an obvious margin. In contrast, our cosine-based quantization works quite robust, achieving almost the same performance in all configurations with very close performance to float32-based training. We conclude that the linear quantization can work well in many cases, but it has the risk of unstable training when low-bits compression is applied.

In addition, we compare different methods in low-bits compression. Because 8- and 4-bits quantization achieves similar results in the above study, we focus on comparing the 2-bits case and apply Hadamard random rotations to improve the linear quantization [40, 17]. As shown in Figure 8 (a), even though the linear quantization can be improved, it still has a margin to our 2-bits compression and float32 in performance and convergence speed. Furthermore, we compare our methods to the 1-bit compression, including signSGD [4], signSGD+Norm [43] and EF-signSGD [15] in Figure 8 (b). In particular, signSGD+Norm is a degenerated version of our method in 1-bit. For our 2-bits and linear 2-bits, we apply a 50% random sparsification [17], which leads to 1-bit per-parameter compression in average. Here, we highlight the following points: (1) signSGD works

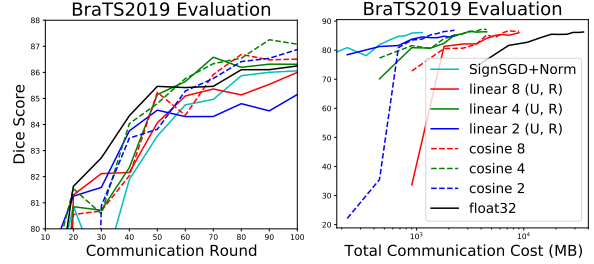


Figure 9: Comparison results (%) to other methods on BraTS2019 dataset ($B = 3, E = 3, C = 1$). Dice scores are shown at different communication rounds and total costs for gradients.

well before 1700 rounds, however, it is finally not converged. We reason this from the inaccurate gradients fail to update the model effectively, and the momentum in the optimizer leads to the failure of training. (2) Even though error feedback has been shown successfully in many previous works [15, 35], a problem needs to be addressed that the current model status may not match well with gradient residual accumulation in history because a worker is not trained in every round. The last update of a local worker can be very far from the current step in federated learning, which has a potential risk of losing gradient precision and achieves limited improvements in Figure 8. (3) As our 1-bit case, signSGD+Norm works stable but it achieves slight worse results compared to the combination of 2-bits quantization and 50% sparsification (84% vs. 85%), which results in the same communication costs.

Figure 9 shows the results of BraTS2019. From the above experiments, we only compare the unbiased version with Hadamard rotations [17]. Consistent with MNIST and CIFAR-10, we also achieve better results in brain tumor semantic segmentation compared to others. Besides, we are interested in the model performance over the transferred data volume, which clearly indicates the necessity of compressing gradients. As a result, it motivates us to pursue extremely high compressed communication while preserving the model performance.

5.3. Combination with gradient sparsification

Gradient sparsification performed on top of quantization so that the two types of methods are combined to reduce the cost further. In these experiments, we leverage the random sparsification [17] on the quantized gradients. We show the results on CIFAR-10 and BraTS2019 in Figure 10 with 25%, 10% and 5% returned gradients. Due to the challenges in this case, we apply the improved probabilistic unbiased quantization with random Hadamard rotations [17] as the baseline. From this figure, we can see the unstable training of linear quantization [17]. In CIFAR-10, even though the 8- and 4-bits compressions achieve similar results with the

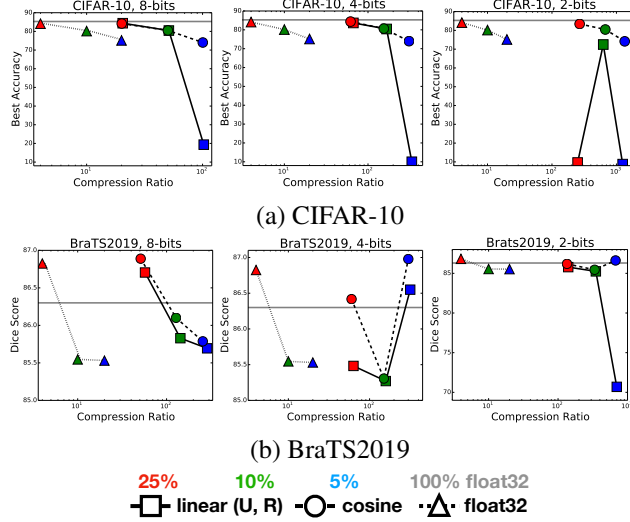


Figure 10: Comparison results (%) on the combination of random sparsification [17]. probabilistic unbiased quantization and Hadamard matrices based random rotation are applied. The logarithmic scale for x-axis is used.

Table 1: Ablation study of more computing clients on CIFAR-10 with 5% random sparsification w.r.t. cost compression ratio and accuracy. Two systems ($B=50$, $E=1$, $C=0.5$) and ($B=50$, $E=5$, $C=0.1$) access the same number of training data. Float32 full training has $\sim 85\%$ accuracy. We report the ratio as $\frac{\text{cost for } (B=50, E=1, C=0.5, 100\%, \text{float32})}{\text{cost for the setups in below}}$.

| Method | (B=50, E=5, C=0.1) | | | (B=50, E=1, C=0.5) | | |
|----------------------|--------------------|-------------|------|--------------------|-------------|-------------|
| | Total cost | Single cost | Acc. | Total cost | Single cost | Acc. |
| float32 | 20 | 20 | 75.2 | 4 | 20 | 82 |
| linear 2 (U, R) [17] | 1250 | 1250 | 8.8 | 243 | 1213 | 69.1 |
| cosine 2 (Ours) | 1344 | 1344 | 74.2 | 259 | 1295 | 82.5 |

entire gradient vector updates, similarly in Figure 6 and 7, they fail to converge the training in the 5% case. Besides, the baseline fails to train a model with 25% 2-bits based gradients, whereas it obtains a model with 10% gradients. We interpret this as the unstable training because of the imprecise gradients from quantization. In contrast, our nonlinear quantization can work well in all the cases, which have the almost same performance as float32-based training, but reduce the communications by $400\times$ to $1200\times$ using 2-bits in CIFAR-10. Additionally, higher dice scores in BraTS2019 can be observed for most cases from our quantization. We also highlight all the models with cosine quantization obtain similar performance to float32 based training, but 2-bits linear quantization with 5% sparsification degenerates significantly.

Table 2: Ablation study on clipping top gradients for the proposed quantization on CIFAR-10 with random sparsification, same as Figure 10. We report the best accuracy. “f32” and “0” means float32 or the original bound is applied.

| Setting | f32 | 0 | 1% | 2% | 3% | 4% | 5% | 6% |
|--------------|------|------|------|------|-------------|-------------|-------------|-------------|
| 8-bits (10%) | 80.2 | 80.5 | 80.5 | 80.6 | 81.3 | 81.6 | 81.0 | 81.3 |
| 2-bits (5%) | 75.2 | 10 | 74.2 | 75.2 | 75.3 | 76.0 | 76.7 | 77.1 |

5.4. Ablation study

First, we make efforts in understanding and showing stronger results with the 5% sparsification on CIFAR-10. Even our 2-bits quantization is able to train a model with more than $1000\times$ compression ratio, there is still a clear gap to the non-compressed training (74.2% vs. 85%). Intuitively, the clients are not enough in each training round. There are 10 clients updating with 5% gradients. From the probabilistic perspective, there are 50% gradients on the server are 0, which limits successful training. Therefore, we conduct an experiment with a different federated configuration of ($B=50$, $E=1$, $C=0.5$). Compared to the previous configuration, the new setup let more clients update, therefore, all the model parameters get updated very likely. Besides, we emphasize that those two setups have similar per-client communication costs. We also point out the new setup is computation-friendly with less training epochs on single node ($E = 1$). In this way, we significantly improve the accuracy from 74.2% to 82.5%, which is even slightly better than the float32-based result 82%.

Second, we set the various angle bounds for quantization with manually gradient clipping, in addition to the bound from the original gradient distribution, as described in section 3. We test the 8- and 2-bits compressions, which are the most precise and coarse quantization in our work. Besides, we test the models on the challenging random sparsification cases, as listed in Table 2. From this table, increasing the clipping bound helps in achieving higher performance. Even though the gradients become less precise when we perform gradient clipping for the largest ones, the clipping helps quantization perform better on the middle-level gradients, which cannot be ignored and more densely distributed. The largest dimension in a gradient vector is typically distributed far from others. Therefore, clipping those gradients is helpful to overall improvements, which demonstrates our motivation for applying manually clipping.

6. Conclusion

We have studied gradient compression in this work, focusing on the quantization. Considering the importance of gradients distributed at different magnitudes, we design a novel gradient quantization method for compressed stochastic gradient descent in the federated setting for dis-

tributed and synchronous learning. Our solution is rather simple and built on the cosine function, which provides finer quantization intervals for the larger gradients compared to the small ones. Due to its nonlinear property, our quantization allows the compressed gradients to approximate the deepest gradient directions, which outperforms linear quantization and their improved versions. In addition to linear quantization, we also show our method is a generalization of previous binary-based optimization [4], enabling precision options of gradients, and achieving strong performance as well as training stability.

Additionally, we show the quantization operation is in particular suitable to use the data-driven compression than float number itself. As a result, we further reduce the communication cost using the *Deflate* algorithm without losing any performance. This is an instance of co-design where learning, quantization, compression are interlinked, which provides ample opportunities for further investigations.

Eventually, our method able to reach more than $1000 \times$ compression in updating the gradients for each client. We believe our quantization is able to work in wider distributed learning scenarios and applications under limited communication constraints, even though we explore our research in the federated learning on image classification and segmentation. We see our contribution as a significant step towards a larger goal that is to communicate less information than it is stored on each client.

Acknowledgement

This work is partially funded by the Helmholtz Association within the project "Trustworthy Federated Data Analytics (TFDA)" (ZT-I-OO1 4).

References

- [1] Alham Fikri Aji and Kenneth Heafield. Sparse communication for distributed gradient descent. *arXiv preprint arXiv:1704.05021*, 2017. 2
- [2] Dan Alistarh, Demjan Grubic, Jerry Li, Ryota Tomioka, and Milan Vojnovic. Qsgd: Communication-efficient sgd via gradient quantization and encoding. In *NeurIPS*, 2017. 1, 2, 3, 5, 6, 7
- [3] Dan Alistarh, Torsten Hoefler, Mikael Johansson, Nikola Konstantinov, Sarit Khirirat, and Cédric Renggli. The convergence of sparsified gradient methods. In *NeurIPS*, pages 5973–5983, 2018. 2
- [4] Jeremy Bernstein, Yu-Xiang Wang, Kamyar Azizzadenesheli, and Animashree Anandkumar. signsdg: Compressed optimisation for non-convex problems. In *ICML*, 2018. 1, 3, 4, 5, 7, 9
- [5] Google AI Blog. *Federated Learning: Collaborative Machine Learning without Centralized Training Data*, 2017. <https://ai.googleblog.com/2017/04/federated-learning-collaborative.html>. 1
- [6] Keith Bonawitz, Hubert Eichner, Wolfgang Grieskamp, Dzmitry Huba, Alex Ingerman, Vladimir Ivanov, Chloe Kiddon, Jakub Konečný, Stefano Mazzocchi, H Brendan McMahan, et al. Towards federated learning at scale: System design. *arXiv preprint arXiv:1902.01046*, 2019. 2
- [7] Chia-Yu Chen, Jiamin Ni, Songtao Lu, Xiaodong Cui, Pin-Yu Chen, Xiao Sun, Naigang Wang, Swagath Venkataramani, Vijayalakshmi Viji Srinivasan, Wei Zhang, et al. Scalecom: Scalable sparsified gradient compression for communication-efficient distributed training. *NeurIPS*, 2020. 2
- [8] Özgün Çiçek, Ahmed Abdulkadir, Soeren S Lienkamp, Thomas Brox, and Olaf Ronneberger. 3d u-net: learning dense volumetric segmentation from sparse annotation. In *MICCAI*, 2016. 6
- [9] Matthieu Courbariaux, Yoshua Bengio, and Jean-Pierre David. Binaryconnect: Training deep neural networks with binary weights during propagations. In *NeurIPS*, 2015. 2
- [10] Peter Deutsch. Deflate compressed data format specification version 1.3. *IETF RFC 1951*, 1996. 2, 5
- [11] Song Han, Huizi Mao, and William J Dally. Deep compression: Compressing deep neural networks with pruning, trained quantization and huffman coding. In *ICLR*, 2016. 2
- [12] Andrew Hard, Kanishka Rao, Rajiv Mathews, Swaroop Ramaswamy, Françoise Beaufays, Sean Augenstein, Hubert Eichner, Chloé Kiddon, and Daniel Ramage. Federated learning for mobile keyboard prediction. *arXiv preprint arXiv:1811.03604*, 2018. 2
- [13] Peter Kairouz, H Brendan McMahan, Brendan Avent, Aurélien Bellet, Mehdi Bennis, Arjun Nitin Bhagoji, Keith Bonawitz, Zachary Charles, Graham Cormode, Rachel Cummings, et al. Advances and open problems in federated learning. *arXiv preprint arXiv:1912.04977*, 2019. 2
- [14] Sai Praneeth Karimireddy, Martin Jaggi, Satyen Kale, Mehryar Mohri, Sashank J Reddi, Sebastian U Stich, and Ananda Theertha Suresh. Mime: Mimicking centralized stochastic algorithms in federated learning. *arXiv preprint arXiv:2008.03606*, 2020. 2
- [15] Sai Praneeth Karimireddy, Quentin Rebjock, Sebastian U Stich, and Martin Jaggi. Error feedback fixes signsdg and other gradient compression schemes. *NeurIPS*, 2019. 1, 3, 5, 7
- [16] Diederik P Kingma and Jimmy Ba. Adam: A method for stochastic optimization. In *ICLR*, 2015. 5
- [17] Jakub Konečný, H Brendan McMahan, Felix X Yu, Peter Richtárik, Ananda Theertha Suresh, and Dave Bacon. Federated learning: Strategies for improving communication efficiency. *arXiv preprint arXiv:1610.05492*, 2016. 1, 2, 3, 5, 7, 8
- [18] Kavya Kopparapu, Eric Lin, and Jessica Zhao. Fedcd: Improving performance in non-iid federated learning. In *SIGKDD*, 2020. 2
- [19] Anusha Lalitha, Osman Cihan Kilinc, Tara Javidi, and Farnaz Koushanfar. Peer-to-peer federated learning on graphs. *arXiv preprint arXiv:1901.11173*, 2019. 2
- [20] Tian Li, Anit Kumar Sahu, Ameet Talwalkar, and Virginia Smith. Federated learning: Challenges, methods, and future directions. *IEEE Signal Processing Magazine*, 2020. 1, 2

[21] Wei Yang Bryan Lim, Nguyen Cong Luong, Dinh Thai Hoang, Yutao Jiao, Ying-Chang Liang, Qiang Yang, Dusit Niyato, and Chunyan Miao. Federated learning in mobile edge networks: A comprehensive survey. *IEEE Communications Surveys & Tutorials*, 2020. 2

[22] Yujun Lin, Song Han, Huiyi Mao, Yu Wang, and Bill Dally. Deep gradient compression: Reducing the communication bandwidth for distributed training. In *ICLR*, 2018. 2, 4

[23] Zechun Liu, Baoyuan Wu, Wenhan Luo, Xin Yang, Wei Liu, and Kwang-Ting Cheng. Bi-real net: Enhancing the performance of 1-bit cnns with improved representational capability and advanced training algorithm. In *ECCV*, 2018. 2

[24] Ilya Loshchilov and Frank Hutter. Sgdr: Stochastic gradient descent with warm restarts. In *ICLR*, 2017. 6

[25] Brendan McMahan, Eider Moore, Daniel Ramage, Seth Hampson, and Blaise Aguera y Arcas. Communication-efficient learning of deep networks from decentralized data. In *AISTATS*, 2017. 1, 2, 3, 5, 6

[26] Bjoern H Menze, Andras Jakab, Stefan Bauer, Jayashree Kalpathy-Cramer, Keyvan Farahani, Justin Kirby, Yuliya Burren, Nicole Porz, Johannes Slotboom, Roland Wiest, et al. The multimodal brain tumor image segmentation benchmark (brats). *IEEE transactions on Medical Imaging*, 2014. 6

[27] Shuo Ouyang, Dezun Dong, Yemao Xu, and Liquan Xiao. Communication optimization strategies for distributed deep learning: A survey. *arXiv preprint arXiv:2003.03009*, 2020. 2

[28] Adam Paszke, Sam Gross, Francisco Massa, Adam Lerer, James Bradbury, Gregory Chanan, Trevor Killeen, Zeming Lin, Natalia Gimelshein, Luca Antiga, et al. Pytorch: An imperative style, high-performance deep learning library. In *NeurIPS*, 2019. 5

[29] Shiva Raj Pokhrel and Jinho Choi. Federated learning with blockchain for autonomous vehicles: Analysis and design challenges. *IEEE Transactions on Communications*, 2020. 2

[30] Sashank Reddi, Zachary Charles, Manzil Zaheer, Zachary Garrett, Keith Rush, Jakub Konečný, Sanjiv Kumar, and H Brendan McMahan. Adaptive federated optimization. *arXiv preprint arXiv:2003.00295*, 2020. 2

[31] Herbert Robbins and Sutton Monro. A stochastic approximation method. *The annals of mathematical statistics*, 1951. 5

[32] Abhijit Guha Roy, Shayan Siddiqui, Sebastian Pölsterl, Nasir Navab, and Christian Wachinger. Braintorrent: A peer-to-peer environment for decentralized federated learning. *arXiv preprint arXiv:1905.06731*, 2019. 2

[33] Sebastian Ruder. An overview of gradient descent optimization algorithms. *arXiv preprint arXiv:1609.04747*, 2016. 4

[34] Theo Ryffel, Andrew Trask, Morten Dahl, Bobby Wagner, Jason Mancuso, Daniel Rueckert, and Jonathan Passerat-Palmbach. A generic framework for privacy preserving deep learning. *arXiv preprint arXiv:1811.04017*, 2018. 5

[35] Frank Seide, Hao Fu, Jasha Droppo, Gang Li, and Dong Yu. 1-bit stochastic gradient descent and its application to data-parallel distributed training of speech dnns. In *Fifteenth Annual Conference of the International Speech Communication Association*, 2014. 3, 7

[36] Micah J Sheller, Brandon Edwards, G Anthony Reina, Jason Martin, Sarthak Pati, Aikaterini Kotrotsou, Mikhail Milchenko, Weilin Xu, Daniel Marcus, Rivka R Colen, et al. Federated learning in medicine: facilitating multi-institutional collaborations without sharing patient data. *Scientific reports*, 2020. 2, 6

[37] Micah J Sheller, G Anthony Reina, Brandon Edwards, Jason Martin, and Spyridon Bakas. Multi-institutional deep learning modeling without sharing patient data: A feasibility study on brain tumor segmentation. In *International MICCAI Brainlesion Workshop*, pages 92–104. Springer, 2018. 2, 6

[38] GW Stewart and JH Miller. Methods of simultaneous iteration for calculating eigenvectors of matrices. *Topics in Numerical Analysis II*, 1975. 2

[39] Nikko Strom. Scalable distributed dnn training using commodity gpu cloud computing. In *Sixteenth Annual Conference of the International Speech Communication Association*, 2015. 2

[40] Ananda Theertha Suresh, X Yu Felix, Sanjiv Kumar, and H Brendan McMahan. Distributed mean estimation with limited communication. In *ICML*, 2017. 1, 2, 3, 5, 7

[41] Ilya Sutskever, James Martens, George Dahl, and Geoffrey Hinton. On the importance of initialization and momentum in deep learning. In *ICML*, 2013. 5

[42] Tensorflow team. *Tensorflow convolutional neural networks tutorial*, 2016. http://www.tensorflow.org/tutorials/deep_cnn. 6

[43] Thijs Vogels, Sai Praneeth Karimireddy, and Martin Jaggi. Powersgd: Practical low-rank gradient compression for distributed optimization. In *NeurIPS*, 2019. 2, 5, 7

[44] Jianqiao Wangni, Jialei Wang, Ji Liu, and Tong Zhang. Gradient sparsification for communication-efficient distributed optimization. In *NeurIPS*, 2018. 2

[45] Wei Wen, Cong Xu, Feng Yan, Chunpeng Wu, Yandan Wang, Yiran Chen, and Hai Li. Terngrad: Ternary gradients to reduce communication in distributed deep learning. In *NeurIPS*, 2017. 2, 3

[46] Qiang Yang, Yang Liu, Tianjian Chen, and Yongxin Tong. Federated machine learning: Concept and applications. *ACM Transactions on Intelligent Systems and Technology (TIST)*, 2019. 2

[47] Timothy Yang, Galen Andrew, Hubert Eichner, Haicheng Sun, Wei Li, Nicholas Kong, Daniel Ramage, and Françoise Beaufays. Applied federated learning: Improving google keyboard query suggestions. *arXiv preprint arXiv:1812.02903*, 2018. 2

[48] Dongqing Zhang, Jiaolong Yang, Dongqiangzi Ye, and Gang Hua. Lq-nets: Learned quantization for highly accurate and compact deep neural networks. In *ECCV*, 2018. 2, 4